Structural Engineering and Mechanics, *Vol. 59, No. 6 (2016) 973-992*
DOI: http://dx.doi.org/10.12989/sem.2016.59.6.973

Displacement and force control of complex element structures by Matrix Condensation

Najmadeen M. Saeed*[1] and Alan S.K. Kwan[2a]

[1]*Civil Engineering Department, University of Raparin, Rania, Kurdistan Region, Iraq*
[2]*Cardiff School of Engineering, Cardiff University, Cardiff CF24 3AA, U.K.*

(Received February 7, 2016, Revised April 10, 2016, Accepted April 15, 2016)

Abstract. A direct and relatively simple method for controlling nodal displacements and/or internal bar forces has been developed for prestressable structural assemblies including complex elements ("macro-elements", e.g., the pantographic element), involving Matrix Condensation, in which structural matrices being built up from matrices of elementary elements. The method is aimed at static shape control of geometrically sensitive structures. The paper discusses identification of the most effective bars for actuation, without incurring violation in bar forces, and also with objective of minimal number of actuators or minimum actuation. The advantages of the method is that the changes for both force and displacement regimes are within a single formulation. The method can also be used for adjustment of bar forces to either reduce instances of high forces or increase low forces (e.g., in a cable nearing slack).

Keywords: force method; matrix condensation; static shape control; displacement control; bar force control; actuator placement; actuation

1. Introduction

The construction industry, by the scale of typical projects and the more imprecise nature of loadings, usually works to a less exacting standard of tolerance than most branches of engineering. Nonetheless, there are applications of structural engineering where tolerances of structural shape and internal forces, under changing service conditions, are not only important but actually impinge on the structure's serviceability limit state. On the other hand, structures composed of beam members such as cable-stayed bridges could undergo a big deflection under the load or may be required to control internal force of a specific cable. In this case, the displacement must be restored and/or the cable force must be controlled and limited according to the desired target. In addition, the application of pantographic structures, which are made from pantographic units that consist of two coplanar, straight beams, joined by a shear connector, could be very delicate and sensitive to distortion.

The process of small changes or movements that improves the current performance or achieves a desired outcome is called an adjustment or control. Shape control can be defined as reduction or

*Corresponding author, Ph.D., E-mail: Najmadeen_qasre@Raparinuni.org
[a]Ph.D., E-mail: Kwan@cardiff.ac.uk

http://www.techno-press.org/?journal=sem&subpage=8 ISSN: 1225-4568 (Print), 1598-6217 (Online)

even elimination of the structural deformation caused by external disturbances (Ziegler 2005). Therefore, some structures are designed to have the ability of changing their shapes by adjusting some of the member lengths or forces (Shea *et al.* 2002). The controlling or adjustment process in structural engineering can be done via elongations of active members capable of length extension/contraction. The element elongations can be done using devices embedded in these members, called actuators, which produce the length extension/contraction (Haftka and Adelman 1985a, Haftka and Adelman 1985b, Edberg 1987, Burdisso and Haftka 1990, Kwan and Pellegrino 1993, Du *et al.* 2013). Earlier and recent studies on the structural control have been reviewed and studied in detail (Burdisso and Haftka 1990, Ziegler 2005, Korkmaz 2011), while a detailed discussion and review on shape control with piezoelectric actuators were presented by Irschik (2002), and Sunar and Rao (1999).

Although the concept of length actuation as the cause of static shape change is simple, work on the associated analytical/computational techniques is not extensive. Haftka and Adelman (1985a) studied shape control by thermal effects, and also via placement of actuators (1985b) with heuristic search. Such indirect approaches have also been tested, e.g., by Subramanian and Mohan (1996) with an algorithm of successive correction based on heuristics. In addition, simulated annealing in combination with a linear finite-element evaluation of control of a precision truss structure was used by Salama *et al.* (1993). You (1997) on the other hand dealt with the problem directly, and showed the direct link between length actuations and displacements for prestressed structures. Kwan & Pellegrino (1993) provided methods to calculate actuations to generate a desired pattern of bar force (i.e. prestress state), but did not address displacements. On the control of both shape and internal forces, little work has been done. An analytical scheme of shape and stress control of pin-jointed prestressed truss structures without external load, using a linear force method of analysis, was investigated by Kawaguchi *et al.* (1996). Overall, far more attention has been paid to dynamic, than static, shape control, as can be gleaned from the survey by Irschik (2002).

Shape control has been done on the different types of structures in order to nullify the distortion of the shape of structure for instance the shape control of beam (Yang and Ngoi 2000, Hadjigeorgiou *et al.* 2006, Yu *et al.* 2009), cable mesh antennas (Mitsugi *et al.* 1990, Tanaka and Natori 2004, Tanaka and Natori 2006, Tanaka 2011, Wang *et al.* 2013, Du *et al.* 2014), intelligent structures (Wang *et al.* 1997), truss structure (Trak and Melosh 1992), and Tensegrity structures (Shea *et al.* 2002).

The purpose of this paper is theoretical direct nodal displacement and internal bar force control and simultaneous nodal displacement and internal bar force control of structures made up of more complex structural components (i.e., those with "macro-elements") via a direct relationship between bar length actuations and the nodal displacements and/or bar forces.

2. Controlling equations utilizing matrix condensation

The previous works have described shape adjustment for a structure made of simple elements. Their examples mostly concern only large space structures (Haftka and Adelman 1985b), beam by piezoelectric actuator (Yang and Ngoi 2000), tension stabilized truss structure (Kawaguchi *et al.* 1996), cable mesh space antennas (Kawaguchi *et al.* 1996, Tanaka and Natori 2004, Tanaka 2011, Du *et al.* 2014), intelligent structures with distributed piezoelectric sensors/actuators (Wang *et al.* 1997) and prestressed cable structures (You 1997). Whereas Saeed's (Saeed 2014) example concern only pin-jointed trusses with bar elements, the same equations and techniques can be

applied also to other structures with elementary elements (e.g., rigidly jointed frames, or plated structures). Structures made up of more complicated structural components (i.e., those with "macro-elements"), e.g., the pantographic element in Section 5.2 have their structural matrices built up from matrices of elementary elements, but the building also involves "Matrix Condensation" in the process. The governing equations for shape adjustment are thus re-derived in this paper, for structures with macro-elements.

2.1 Matrix Condensation

Matrix Condensation is a technique of reducing the size and simplification of the structural matrices (equilibrium, compatibility and flexibility matrices) in the force method equations of structural analysis by condensing out unloaded degrees of freedom (Pellegrino *et al*. 1992). The current technique is founded in the force method to allow "easy access" to the contributing parameters affecting the internal forces and the external displacements. This condensation facility allows "macro-elements" to be built up from elementary elements, where the connectivity between the elementary elements form unloaded "internal joints" within the macro-elements which can then be "condensed out" (Kwan and Pellegrino 1994). The system of equilibrium, compatibility and flexibility should be in the form of Fig. 1.

In the Force Method (Kwan 1991, Pellegrino *et al.* 1992, Pellegrino 1993) , the relation between the generalized internal bar force **t** and the generalized external nodal load **p** is the equilibrium matrix **A** as

$$\mathbf{A}\mathbf{t} = \mathbf{p} \tag{1}$$

In addition, the generalized internal bar elongation **e** due to **t** are related to the generalized external nodal displacements **d** (due to **p**) by compatibility matrix **B**, because of the linear equations of compatibility as

$$\mathbf{B}\mathbf{d} = \mathbf{e} \tag{2}$$

Lastly, the flexibility relationships involving the flexibility matrix **F** are as

$$\mathbf{F}\mathbf{t} = \mathbf{e} \tag{3}$$

For an *i*-dimensional structural assembly with *b* bar and *j* joints, it is likely that some of the nodal forces are always equal to zero. The equilibrium equations relating to these zero load components can be condensed out from immediate consideration, and similarly the corresponding displacement components and compatibility equations can also be condensed out as well, thus leaving a smaller set of equations. Similarly, when "macro-elements" are built up from elementary elements, the unloaded "internal" joints within the macro-elements present equations for condensation. Consider $(m+p)$-dimensional vectors of external joint load **p** and displacement **d**, and $(n+p)$-dimensional vectors of internal bar force **t** and bar elongation **e**, where the load vector **p** is partitioned into the two sub-vectors $\mathbf{p}_m$ with *m* non-zero components and the remaining $\mathbf{p}_p$ with *p* zero components. Similarly, the vector of displacements **d** can also be partitioned into $\mathbf{d}_m$ and $\mathbf{d}_p$ sub-vectors where $\mathbf{d}_m$ and $\mathbf{d}_p$ correspond directly to $\mathbf{p}_m$ and $\mathbf{p}_p$ respectively, as shown in Fig. 1(a) and (b).

The equilibrium matrix can be re-arranged with simple row-exchange so that the equations corresponding to zero loads appear in the lower *p* equations, and hence $\mathbf{p}_m$ and $\mathbf{p}_p$ contain only (non-zero) and (zero) load components respectively. Partitioning can then be carried on the

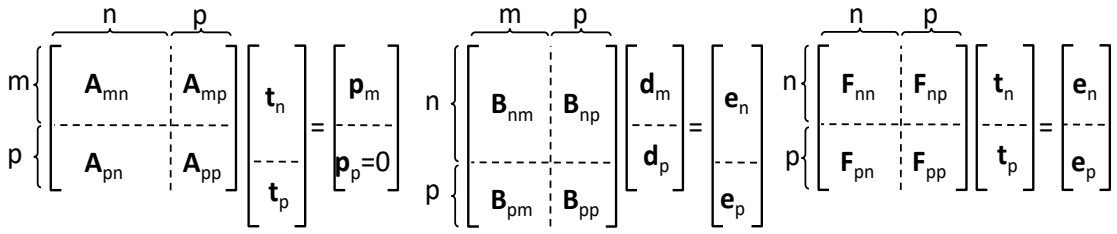

(a) (b) (c)

Fig. 1 Partitioned forms of the systems of (a) equilibrium, (b) compatibility and (c) flexibility equations. Adapted from Pellegrino *et al*. (1992)

equilibrium matrix as shown in Fig. 1(a). Due to the correspondence between components of load and displacement, the compatibility matrix can also be re-arranged in a similar way with column-exchanges corresponding exactly to the row-exchanges of the equilibrium matrix. In this way, the $\mathbf{B}_{nm}$ sub-matrix in Fig. 1(b) is still the transpose of the equilibrium sub-matrix $\mathbf{A}_{mn}$ in Fig. 1(a). Furthermore, the same row- and column exchanges must also be carried out in the flexibility matrix so that the $\mathbf{t}_n$, $\mathbf{e}_n$, etc. in Fig. 1(c) correspond to the internal forces and displacements in the equilibrium and compatibility relationships in Fig. 1(a) and (b).

The reduced matrices can be obtained from the following process (Pellegrino *et al.* 1992). Firstly, the system of equilibrium equations after reduction of the equilibrium matrix by condensing out *p* rows with corresponding *p* load components is

$$\mathbf{A}^* \mathbf{t}^* = \mathbf{p}^* \tag{4}$$

where $\mathbf{A}^*$ is the reduced equilibrium matrix which relates the *m* non-vanishing (non-zero) load components to *n* (almost) arbitrary chosen condensed generalized internal bar forces. Since the lower *p* equation of $\mathbf{A}$ are homogeneous, $\mathbf{A}_{pn}\mathbf{t}_n + \mathbf{A}_{pp}\mathbf{t}_p = \mathbf{0}$, i.e., $\mathbf{t}_p = -\mathbf{A}_{pp}^{-1}\mathbf{A}_{pn}\mathbf{t}_n$, which can be used as substitution for $\mathbf{t}_p$ in $\mathbf{A}_{mn}\mathbf{t}_n + \mathbf{A}_{mp}\mathbf{t}_p = \mathbf{p}_m$, to give $\mathbf{A}_{mn}\mathbf{t}_n - \mathbf{A}_{mp}\mathbf{A}_{pp}^{-1}\mathbf{A}_{pn}\mathbf{t}_n = \mathbf{p}_m$, i.e., $\left(\mathbf{A}_{mn} - \mathbf{A}_{mp}\mathbf{A}_{pp}^{-1}\mathbf{A}_{pn}\right)\mathbf{t}_n = \mathbf{p}_m$ and hence

$$\mathbf{A}^* = \mathbf{A}_{mn} - \mathbf{A}_{mp}\mathbf{A}_{pp}^{-1}\mathbf{A}_{pu} \tag{5}$$

$\mathbf{t}^*$ is the generalized internal bar forces and is equal to $\mathbf{t}_n$, and $\mathbf{p}^*$ is the generalized external (non-zero) load and equal to $\mathbf{p}_m$. The size of reduced equilibrium matrix $\mathbf{A}^*$ is *m* by *n*.

Secondly, the system of compatibility equations "mirrors" the reduction in equilibrium equations, by condensing out *p* columns corresponding to the *p* displacements components and *p* rows corresponding to *p* generalized internal bar elongation, resulting in

$$\mathbf{B}^* \mathbf{d}^* = \mathbf{e}^* \tag{6}$$

where $\mathbf{d}^*$ is the generalized external nodal displacement (and equal to $\mathbf{d}_m$) and $\mathbf{B}^*$ is the reduced compatibility matrix relating the *m* joint displacements (corresponding to the *m* non-zero load components) to the *n* chosen condensed generalized internal bar elongation (corresponding to the chosen generalized internal bar force)

$$\mathbf{B}^{*} = \mathbf{A}_{\mathbf{mn}}^{\mathbf{T}} - \mathbf{A}_{\mathbf{pn}}^{\mathbf{T}} (\mathbf{A}_{\mathbf{pp}}^{\mathbf{T}})^{-1}\ \mathbf{A}_{\mathbf{mp}}^{\mathbf{T}} \tag{7}$$

The matrix **B*** thus has size *n* by *m*. From Eqs. (5) and (7)

$$\mathbf{B}^{*} = (\mathbf{A}^{*})^{\mathbf{T}} \tag{8}$$

The vector $\mathbf{e}^{*}$ is the condensed generalized internal bar elongation corresponding to the chosen generalized internal bar force

$$\mathbf{e}^{*} = \mathbf{e}_{\mathbf{n}} - \mathbf{A}_{\mathbf{pn}}^{\mathbf{T}} (\mathbf{A}_{\mathbf{pp}}^{\mathbf{T}})^{-1}\ \mathbf{e}_{\mathbf{p}} \tag{9}$$

where $\mathbf{e}_{\mathbf{p}}$ is the generalized internal bar elongation corresponding to the generalized internal bar force $\mathbf{t}_{\mathbf{p}}$.

$$\mathbf{t}_{\mathbf{p}} = -(\mathbf{A}_{\mathbf{pn}})^{-1}\, \mathbf{A}_{\mathbf{pn}}\ \mathrm{t}_{\mathbf{n}} \tag{10}$$

Substituting Eq. (7) into Eq. (6) yields

$$\mathbf{B}^{*}\, \mathbf{d}_{\mathbf{m}} = \mathbf{e}^{*} \tag{11}$$

Pellegrino *et al.* (1992) also found the components of external displacement $\mathbf{d}_{\mathbf{p}}$, which are the displacements corresponding to the zero load components $\mathbf{p}_{\mathbf{p}}$ (=**0**)

$$\mathbf{d}_{\mathbf{p}} = (\mathbf{A}_{\mathbf{pp}}^{\mathbf{T}})^{-1}\, \mathbf{e}_{\mathbf{p}} - (\mathbf{A}_{\mathbf{pp}}^{\mathbf{T}})^{-1}\ \mathbf{A}_{\mathbf{mp}}^{\mathbf{T}}\, \mathbf{d}_{\mathbf{m}} \tag{12}$$

Finally, the condensed system of flexibility equations is

$$\mathbf{F}^{*}\, \mathbf{t}^{*} = \mathbf{e}^{*} \tag{13}$$

where $\mathbf{F}^{*}$ the reduced flexibility matrix is given by

$$\mathbf{F}^{*} = \mathbf{F}_{\mathbf{nn}} - \mathbf{A}_{\mathbf{pp}}^{-1}\, \mathbf{A}_{\mathbf{pn}} - \mathbf{A}_{\mathbf{pn}}^{\mathbf{T}} (\mathbf{A}_{\mathbf{pp}}^{\mathbf{T}})^{-1}\, \mathbf{F}_{\mathbf{pn}} + \mathbf{A}_{\mathbf{pn}}^{\mathbf{T}}\, (\mathbf{A}_{\mathbf{pp}}^{\mathbf{T}})^{-1} \mathbf{F}_{\mathbf{pp}}\, \mathbf{A}_{\mathbf{pp}}^{-1}\, \mathbf{A}_{\mathbf{pn}} \tag{14}$$

and $\mathbf{t}^{*}$ is the internal bar forces (and equal to $\mathbf{t}_{\mathbf{n}}$).
Moreover $\mathbf{e}_{\mathbf{n}}$ and $\mathbf{e}_{\mathbf{p}}$ can be calculated separately through the following equations respectively

$$\mathbf{e}_{\mathbf{n}} = (\mathbf{F}_{\mathbf{nn}} - \mathbf{F}_{\mathbf{np}}\, \mathbf{A}_{\mathbf{pp}}^{-1}\, \mathbf{A}_{\mathbf{pn}})\mathbf{t}_{\mathbf{n}} \tag{15}$$

$$\mathbf{e}_{\mathbf{p}} = (\mathbf{F}_{\mathbf{pn}} - \mathbf{F}_{\mathbf{pp}}\, \mathbf{A}_{\mathbf{pp}}^{-1}\, \mathbf{A}_{\mathbf{pn}})\mathbf{t}_{\mathbf{n}} \tag{16}$$

The general solution of the reduced internal bar force $\mathbf{t}_{\mathbf{n}}$ in the condensed equilibrium equations is the summation of a particular solution (which is a set of bar forces in equilibrium with the load, but not necessarily satisfying compatibility) and the complementary homogeneous solution. The particular solution is *any* vector $\mathbf{t}_{\mathbf{n}}$ that satisfies Eq. (4), and one such vector is $\mathbf{t}_{\mathbf{nH}}$ obtained from $\mathbf{t}_{\mathbf{nH}} = \left(\mathbf{A}^{*}\right)^{+} \mathbf{p}_{\mathbf{m}}$ where $\left(\mathbf{A}^{*}\right)^{+}$ is the pseudo-inverse of reduced equilibrium matrix.

The complementary homogenous solution is the set of reduced bar forces solutions that satisfies $\mathbf{A}^{*}\, \mathbf{t}_{\mathbf{n}} = \mathbf{0}$, i.e., the set of non-vanishing bar forces in equilibrium with zero external load. This is readily calculated by the nullspace $(\mathbf{A}^{*}) = \mathbf{S}^{*}$, and $\mathbf{S}^{*}$ is the condensed states of self-stress. The number of such condensed states of self-stress depends on the statical redundancy s^{*} of

the indeterminate structure (*note:* the determinate structure there has no states of self-stress). The expression of $\mathbf{S}^*\boldsymbol{\alpha}^*$ is thus the complementary homogeneous solution, where $\boldsymbol{\alpha}^*$ is a vector of s^* coefficients reflecting a set of combinatorial constants (that has to be determined through satisfaction of compatibility). The total general solution for condensed equilibrium equation is thus combining a particular solution and the complementary solution, consequently

$$\mathbf{t_n} = \mathbf{t_{nH}} + \mathbf{S}^* \boldsymbol{\alpha}^* \tag{17}$$

A structure can in general have lack of fit due to initial construction imperfection, or temperature change, or, as in our purpose, deliberate extensional changes to control the displacement and/or internal bar force of the structure. A bar can have axial force due to external load or any of these other "lack of fit" effects. Therefore, the total elongation of the bar is made up of two parts, one part due to axial force of the bar, i.e., $\mathbf{F}^*\mathbf{t_n}$, while the other part $\mathbf{e}_\mathbf{o}^*$ comes from lack of fit (or which can be deliberately introduced to adjust the structure's shape or force distribution). At this point, we introduce a vector of elongation actuation $\mathbf{e}_\mathbf{o}^*$ to each bar. In reality, since elongation actuation greatly complicates the physical makeup of a bar, we would have actuation only for a limited number of bars, and hence many elements of $\mathbf{e}_\mathbf{o}^*$ will remain zero. Currently, we will allow any bar the capacity for actuation, and thus $\mathbf{e}_\mathbf{o}^*$ is fully populated, and Eq. (17) becomes

$$\mathbf{e}^* = \mathbf{e}_\mathbf{o}^* + \mathbf{F}^* \mathbf{t_n} \tag{18}$$

In the current context, $\mathbf{e}_\mathbf{o}^*$, is principally the vector of elongation actuation introduced to each bar for the purpose of adjustment. In the same fashion as Eq. (18), Eqs. (17) and (16) can be re-written to include the lack of fit, and they thus take the following form

$$\mathbf{e_n} = \mathbf{e_{no}} + (\mathbf{F_{nn}} - \mathbf{F_{np}}\ \mathbf{A_{pp}^{-1}}\ \mathbf{A_{pn}})\mathbf{t_n} \tag{19}$$

and

$$\mathbf{e_p} = \mathbf{e_{po}} + (\mathbf{F_{pn}} - \mathbf{F_{pp}}\ \mathbf{A_{pp}^{-1}}\ \mathbf{A_{pn}})\mathbf{t_n} \tag{20}$$

i.e., the total condensed elongation in each condensed bar is the sum of actuation of the condensed bar, and the elongation of the same bar due to axial force. Substitution of Eq. (17) into Eq. (18) thus gives

$$\mathbf{e}^* = \mathbf{e}_\mathbf{o}^* + \mathbf{F}^*(\mathbf{t_{nH}} + \mathbf{S}^*\boldsymbol{\alpha}^*) \tag{21}$$

Compatibility for the set of condensed bar elongations can be assured by it being found in the set of compatible elongations, i.e., in columnspace ($\mathbf{B}^*$), whereas left-nullspace ($\mathbf{B}^*$) contains the basis for all the incompatible condensed bar elongations. Subsequently, the compatibility condition can be imposed by stating that the condensed bar elongations $\mathbf{e}^*$ must be orthogonal to the left-nullspace ($\mathbf{B}^*$) (i.e., by stating that the elongations cannot have any component among the incompatible elongations as found in the left-nullspace). By virtue of $(\mathbf{B}^*)^\mathrm{T}=\mathbf{A}^*$, left-nullspace ($\mathbf{B}^*$) = nullspace ($\mathbf{A}^*$), and since nullspace ($\mathbf{A}^*$) are the states of selfstress, then the compatibility condition is thus that the states of selfstress must be orthogonal to the elongations, i.e., $(\mathbf{S}^*)^\mathrm{T}\ \mathbf{e}^*=\mathbf{0}$, and

$$\mathbf{S}^{*\mathbf{T}}\mathbf{e}_{\mathbf{o}}^{*}+\mathbf{S}^{*\mathbf{T}}\mathbf{F}^{*}(\mathbf{t}_{\mathbf{nH}}+\mathbf{S}^{*}\boldsymbol{\alpha}^{*})=0 \tag{22}$$

and thus

$$-\boldsymbol{\alpha}^{*}=(\mathbf{S}^{*\mathbf{T}}\mathbf{F}^{*}\mathbf{S}^{*})^{-1}[\mathbf{S}^{*\mathbf{T}}\mathbf{e}_{\mathbf{o}}^{*}+\mathbf{S}^{*\mathbf{T}}\mathbf{F}^{*}\mathbf{t}_{\mathbf{nH}}] \tag{23}$$

Through back-substitution with $\boldsymbol{\alpha}^{*}$, we can thus find the structural vectors of $\mathbf{e}^{*}$ (Eq. (21)), $\mathbf{t}_{\mathbf{n}}$ (Eq. (17)) and $\mathbf{d}_{\mathbf{m}}$ (Eq. (11)).

2.2 Displacement control without regard to bar forces

In Section 0, structural analysis was presented utilizing a matrix reduction technique, for structures prestressed with an initial $\mathbf{e}_{\mathbf{o}}$. This reduced matrix technique in the Force Method can now be applied to the process of controlling (imperfect) structural shape. We shall initially be concerned with only displacement control without any concern of associated internal force change in the structure. For controlling displacements $\mathbf{d}_{\mathbf{m}}$ which are not associated with zero loads, we start with substituting Eq. (23) into Eq. (21) to give

$$\mathbf{e}^{*}=\mathbf{e}_{\mathbf{o}}^{*}+\mathbf{F}^{*}(\mathbf{t}_{\mathbf{nH}}-\mathbf{S}^{*}(\mathbf{S}^{*\mathbf{T}}\mathbf{F}^{*}\mathbf{S}^{*})^{-1}[\mathbf{S}^{*\mathbf{T}}\mathbf{e}_{\mathbf{o}}^{*}+\mathbf{S}^{*\mathbf{T}}\mathbf{F}^{*}\mathbf{t}_{\mathbf{nH}}]) \tag{24}$$

and also by substituting Eq. (24) into Eq. (11) to give

$$\mathbf{d}_{\mathbf{m}}=\mathbf{B}^{*+}[\mathbf{e}_{\mathbf{o}}^{*}+\mathbf{F}(\mathbf{t}_{\mathbf{nH}}-\mathbf{S}^{*}(\mathbf{S}^{*\mathbf{T}}\mathbf{F}^{*}\mathbf{S}^{*})^{-1}[\mathbf{S}^{*\mathbf{T}}\mathbf{e}_{\mathbf{o}}^{*}+\mathbf{S}^{*\mathbf{T}}\mathbf{F}^{*}\mathbf{t}_{\mathbf{nH}}]) \tag{25}$$

Eq. (9) showed that $\mathbf{e}^{*}=\mathbf{e}_{\mathbf{n}}-\mathbf{A}_{\mathbf{pu}}^{\mathbf{T}}(\mathbf{A}_{\mathbf{pu}}^{\mathbf{T}})^{-1}\mathbf{e}_{\mathbf{p}}$ and hence, similarly

$$\mathbf{e}^{*}=\mathbf{e}_{\mathbf{no}}-\mathbf{A}_{\mathbf{pu}}^{\mathbf{T}}(\mathbf{A}_{\mathbf{pu}}^{\mathbf{T}})^{-1}\mathbf{e}_{\mathbf{po}} \tag{26}$$

where $\mathbf{e}_{\mathbf{o}}^{*}$ is the condensed generalized internal bar actuation of bar force. Substitution of Eq. (26) into Eq. (25) gives

$$\begin{aligned}\mathbf{d}_{\mathbf{m}}=&[\mathbf{B}^{*+}\mathbf{F}^{*}-\mathbf{B}^{*+}\mathbf{F}^{*}\mathbf{S}^{*}(\mathbf{S}^{*\mathbf{T}}\mathbf{F}^{*}\mathbf{S}^{*})^{-1}\mathbf{S}^{*\mathbf{T}}\mathbf{F}^{*}]\mathbf{t}_{\mathbf{nH}}\\&+[\mathbf{B}^{*+}-\mathbf{B}^{*+}\mathbf{F}^{*}\mathbf{S}^{*}(\mathbf{S}^{*\mathbf{T}}\mathbf{F}^{*}\mathbf{S}^{*})^{-1}\mathbf{S}^{*\mathbf{T}}]\mathbf{e}_{\mathbf{no}}\\&-[\mathbf{B}^{*+}\mathbf{A}_{\mathbf{pn}}^{\mathbf{T}}(\mathbf{A}_{\mathbf{pp}}^{\mathbf{T}})^{-1}-\mathbf{B}^{*+}\mathbf{F}^{*}\mathbf{S}^{*}(\mathbf{S}^{*\mathbf{T}}\mathbf{F}^{*}\mathbf{S}^{*})^{-1}\mathbf{S}^{*\mathbf{T}}\mathbf{A}_{\mathbf{pn}}^{\mathbf{T}}(\mathbf{A}_{\mathbf{pp}}^{\mathbf{T}})^{-1}]\mathbf{e}_{\mathbf{po}}\end{aligned} \tag{27}$$

Eq. (27) can be written in the simpler form

$$\mathbf{d}_{\mathbf{m}}=\mathbf{C}_{1}\mathbf{t}_{\mathbf{nH}}+\mathbf{C}_{2}\mathbf{e}_{\mathbf{no}}+\mathbf{C}_{3}\mathbf{e}_{\mathbf{po}} \tag{28}$$

where $\mathbf{C}_1=\mathbf{C}\,\mathbf{F}^{*}$, $\mathbf{C}_2=\mathbf{C}$, $\mathbf{C}_3=\mathbf{C}\,\mathbf{r}$, $\mathbf{C}=(\mathbf{B}^{*+}-\mathbf{B}^{*}+\mathbf{F}^{*}\mathbf{S}^{*}(\mathbf{S}^{*\mathbf{T}}\mathbf{F}^{*}\mathbf{S}^{*})^{-1}\mathbf{S}^{*\mathbf{T}})$ and $\mathbf{r}=-\mathbf{A}_{\mathbf{pn}}^{\mathbf{T}}\ (\mathbf{A}_{\mathbf{pp}}^{\mathbf{T}})^{-1}$

To calculate $\mathbf{d}_{\mathbf{p}}$, we substitute Eqs. (20) and (28) into Eq. (12) to give

$$\mathbf{d}_{\mathbf{p}}=(\mathbf{A}_{\mathbf{pp}}^{\mathbf{T}})^{-1}[\mathbf{e}_{\mathbf{po}}+(\mathbf{F}_{\mathbf{pn}}-\mathbf{F}_{\mathbf{pp}}\,\mathbf{A}_{\mathbf{pp}}^{-1}\mathbf{A}_{\mathbf{pn}})\mathbf{t}_{\mathbf{n}}]-(\mathbf{A}_{\mathbf{pp}}^{\mathbf{T}})^{-1}\,\mathbf{A}_{\mathbf{mp}}^{\mathbf{T}}[\mathbf{C}_{1}\,\mathbf{t}_{\mathbf{nH}}+\mathbf{C}_{2}\,\mathbf{e}_{\mathbf{no}}+\mathbf{C}_{3}\,\mathbf{e}_{\mathbf{po}}] \tag{29}$$

For ease of presentation, we adapt $\mathbf{v}=\mathbf{F}_{\mathbf{pn}}-\mathbf{F}_{\mathbf{pp}}\,\mathbf{A}_{\mathbf{pp}}^{-1}\,\mathbf{A}_{\mathbf{pn}}$ and then substitute Eqs. (17) and (23) into (29) to give

$$\mathbf{d_p} = (\mathbf{A_{pp}^T})^{-1}[\mathbf{e_{po}} + \mathbf{v}\{\mathbf{t_{nH}} - \mathbf{S^*}(\mathbf{S^{*T}F^*S^*})^{-1}[\mathbf{S^{*T}}e_o^* + \mathbf{S^{*T}}F^* t_{nH}]\}]$$

$$-(\mathbf{A_{pp}^T})^{-1}\,\mathbf{A_{mp}^T}[\mathbf{C}_1\,\mathbf{t_{nH}} + \mathbf{C}_2\,\mathbf{e_{no}} + \mathbf{C}_3\,\mathbf{e_{po}}] \tag{30}$$

Substituting Eq. (26) into Eq. (30), we obtain the condensed displacements $\mathbf{d_p}$, which are the displacements corresponding to the zero load components $\mathbf{p_p}$ (=**0**) as

$$\mathbf{d_p} = (\mathbf{A_{pp}^T})^{-1}[\mathbf{e_{po}} + \mathbf{v}\{\mathbf{t_{nH}} - \mathbf{S^*}(\mathbf{S^{*T}F^*S^*})^{-1}[\mathbf{S^{*T}}(\mathbf{e_{no}} + \mathbf{re_{po}}) + \mathbf{S^{*T}F^*t_{nH}}]\}]$$

$$-(\mathbf{A_{pp}^T})^{-1}\,\mathbf{A_{mp}^T}[\mathbf{C}_1\,\mathbf{t_{nH}} + \mathbf{C}_2\,\mathbf{e_{no}} + \mathbf{C}_3\,\mathbf{e_{po}}] \tag{31}$$

Which can be presented in a simplified form as

$$\mathbf{d_p} = \mathbf{Q}_1\,\mathbf{t_{nH}} + \mathbf{Q}_2\,\mathbf{e_{no}} + \mathbf{Q}_3\,\mathbf{e_{po}} \tag{32}$$

where $\mathbf{Q}_1 = [(\mathbf{A_{pp}^T})^{-1}\,\mathbf{v} - (\mathbf{A_{pp}^T})^{-1}\,\mathbf{v}\,\mathbf{S^*}(\mathbf{S^{*T}F^*S^*})^{-1}\,\mathbf{S^{*T}}\,\mathbf{F^*} - (\mathbf{A_{pp}^T})^{-1}\mathbf{A_{mp}^T}\,\mathbf{CF^*}]$

$\mathbf{Q}_2 = -[(\mathbf{A_{pp}^T})^{-1}\,\mathbf{v}\,\mathbf{S^*}(\mathbf{S^{*T}F^*S^*})^{-1}\,\mathbf{S^{*T}} + (\mathbf{A_{pp}^T})^{-1}\mathbf{A_{mp}^T}\,\mathbf{C}]$

$\mathbf{Q}_3 = -[(\mathbf{A_{pp}^T})^{-1}\,\mathbf{v}\,\mathbf{S^*}(\mathbf{S^{*T}F^*S^*})^{-1}\,\mathbf{S^{*T}}\,\mathrm{r} - (\mathbf{A_{pp}^T})^{-1} + (\mathbf{A_{pp}^T})^{-1}\mathbf{A_{mp}^T}\,\mathbf{Cr}]$ and $\mathbf{v} = \mathbf{F_{pn}} - \mathbf{F_{pp}}(\mathbf{A_{pp}})^{-1}\,\mathbf{A_{pn}}$

Eqs. (28) and (32) provide the non-vanishing and vanishing displacements of the structure respectively, without regard to each other through using the condensed matrix method, due to $\mathbf{t_{nH}}$ and the actuation $\mathbf{e_{no}}$ and $\mathbf{e_{po}}$. Both equations have a great role in calculating displacement of a morphing structure through adjusting bar actuation (rotation), especially Eq. (28) which can be used to provide displacement of non-vanishing displacements of a pantographic morphing aerofoil structure since in the morphing aerofoil structure, only the outer face shape of the aerofoil is significant. Combining together Eqs. (28) and (32), we get:

$$\mathbf{d_c} = \mathbf{d_{pc}} + \mathbf{Y_c}\,\mathbf{e_{oc}} \tag{33}$$

where $\mathbf{d_{pc}}=[\mathbf{C}_1\ \mathbf{Q}_1]^{\mathbf{T}}\ \mathbf{t_{nH}}$ is the vector of nodal displacements of the structure due only to non-vanishing load component, $\mathbf{Y_c}=[\mathbf{Y_n}\ \mathbf{Y_p}]$, $\mathbf{Y_c}=[\mathbf{C}_2\ \mathbf{Q}_2]^{\mathrm{T}}$, $\mathbf{Y_p}=[\mathbf{C}_3\ \mathbf{Q}_3]^{\mathrm{T}}$, $\mathbf{e_{oc}}=[\mathbf{e_{no}}\ \mathbf{e_{po}}]^{\mathrm{T}}$ and $\mathbf{d_c}$ is the resultant nodal displacements after some elongation actuation $\mathbf{e_{oc}}$ has been applied in the condensed matrix method.

2.3 Bar forces control without regard to displacements

Controlling of internal member force of some structures and/or some members are more important than the controlling displacements particularly if the structures have cable members in order to avoid slack of the cables so that the cable must be tightened. Furthermore, slender members of the structures are exposed to buckling with extra load, and in this case the compressive force of those type of member must be reduced. The process of force control can be done only in statically indeterminate structures.

For the equation of non-vanishing bar forces control without regard to displacements, we can start by substituting Eq. (26) into Eq. (17) to give

$$\mathbf{t_n} = \mathbf{t_{nH}} - \mathbf{S^*}(\mathbf{S^{*T}F^*S^*})^{-1}[\mathbf{S^{*T}}(\mathbf{e_{no}} - \mathbf{A_{pn}^T}(\mathbf{A_{pp}^T})^{-1}\mathbf{e_{po}}) + \mathbf{S^{*T}F^*}\ \mathbf{t_{nH}}] \tag{34}$$

with previously defined substitutions $\mathbf{r} = -\mathbf{A}_{\mathbf{pn}}^{\mathbf{T}}(\mathbf{A}_{\mathbf{pp}}^{\mathbf{T}})^{-1}$ and $\mathbf{Q} = \mathbf{S}^{*}(\mathbf{S}^{*\mathbf{T}}\mathbf{F}^{*}\mathbf{S}^{*})^{-1}\mathbf{S}^{*\mathbf{T}}$ (Eqs. (28) and (32)) Eq. (34) can be re-written as

$$\mathbf{t}_{\mathbf{n}} = \mathbf{t}_{\mathbf{nH}} - \mathbf{Q}\,\mathbf{F}^{*}\,\mathbf{t}_{\mathbf{nH}} - \mathbf{Q}\mathbf{e}_{\mathbf{no}} - \mathbf{Q}\mathbf{r}\mathbf{e}_{\mathbf{po}} \tag{35}$$

For controlling $\mathbf{t}_{\mathbf{p}}$ without any regard to displacements, Eq. (28) is substituted into Eq. (32) to give

$$\mathbf{t}_{\mathbf{p}} = \mathbf{J}\mathbf{t}_{\mathbf{nH}} - \mathbf{J}\mathbf{Q}\mathbf{F}^{*}\,\mathbf{t}_{\mathbf{nH}} - \mathbf{J}\mathbf{Q}\mathbf{e}_{\mathbf{no}} - \mathbf{J}\mathbf{Q}\mathbf{r}\mathbf{e}_{\mathbf{po}} \tag{36}$$

where $\mathbf{J} = -(\mathbf{A}_{\mathbf{pp}})^{-1}\,\mathbf{A}_{\mathbf{pn}}$ for ease of viewing. Combination of Eqs. (28) and (32) gives

$$\mathbf{t}_{\mathbf{c}} = \mathbf{t}_{\mathbf{pc}} + \mathbf{Z}_{\mathbf{c}}\,\mathbf{e}_{\mathbf{oc}} \tag{37}$$

where $\mathbf{t}_{\mathbf{pc}} = \begin{bmatrix} \mathbf{t}_{\mathbf{nH}} - \mathbf{Q}\mathbf{F}^{*}\mathbf{t}_{\mathbf{nH}} \\ \mathbf{J}\mathbf{t}_{\mathbf{nH}} - \mathbf{J}\mathbf{Q}\mathbf{F}^{*}\mathbf{t}_{\mathbf{nH}} \end{bmatrix}$ is the vector of bar forces of the structure due only to non-vanishing load components, and $\mathbf{Z}_{\mathbf{c}}=[\mathbf{Z}_{\mathbf{n}}\ \mathbf{Z}_{\mathbf{p}}]$, $\mathbf{Z}_{\mathbf{c}}=[-\mathbf{Q}_2\ -\mathbf{J}\mathbf{Q}]^{\mathrm{T}}$, $\mathbf{Z}_{\mathbf{p}}=[\mathbf{Q}\mathbf{r}\ \mathbf{J}\mathbf{Q}\mathbf{r}]^{\mathrm{T}}$, $\mathbf{e}_{\mathbf{oc}}=[\mathbf{e}_{\mathbf{no}}\ \mathbf{e}_{\mathbf{po}}]^{\mathrm{T}}$, $\mathbf{t}_{\mathbf{c}}$ is the resultant bar forces after some elongation actuation $\mathbf{e}_{\mathbf{oc}}$ has been applied in the condensed matrix method.

2.4 Simultaneous displacement and bar force control

Controls of either joint displacement or the bar force due to the external load without consideration of the other, through using the condensed matrix method are discussed in Sections 0 and 0 respectively. Practically and theoretically, control of one will also have some requirements on the other, or at least monitoring on the other to ensure present limits are not breached. For instance, in a structure with cables, these might have a lower limit on axial force to prevent slack, while other slender strut members will have upper limits to prevent buckling. So while controlling the external nodal displacements of such a structure, it may be necessary to also control the internal bar forces simultaneously via the same set of $\mathbf{e}_{\mathbf{oc}}$. For the purpose of adoption this method, Eqs. (33) and (37) are combined together, to enforce displacement and bar force are satisfied simultaneously

$$\begin{bmatrix} \mathbf{Y}_{\mathbf{c}} \\ \mathbf{Z}_{\mathbf{c}} \end{bmatrix} \mathbf{e}_{\mathbf{oc}} = \begin{bmatrix} \mathbf{d}_{\mathbf{c}} - \mathbf{d}_{\mathbf{pc}} \\ \mathbf{t}_{\mathbf{c}} - \mathbf{t}_{\mathbf{pc}} \end{bmatrix} \tag{38}$$

In this method, because of the typically high number of equations ($ij-c$ in $\mathbf{Y}_{\mathbf{c}}$ and b in $\mathbf{Z}_{\mathbf{c}}$) while there are only b unknowns in $\mathbf{e}_{\mathbf{oc}}$, then Eq. (38) will be over-determinate by many degrees and insoluble. Therefore, only a least-squares "approximation" is possible for $\mathbf{e}_{\mathbf{oc}}$, which is the most appropriate way of obtaining $\mathbf{e}_{\mathbf{o}}$, since it is a common use to compute a 'best fit' (least squares) solution to a system of linear equations and its accuracy is enough for our purpose. This is mainly only of academic interest, and typical situations are under-determinate and allow a choice in $\mathbf{e}_{\mathbf{oc}}$ because in most typical structures the displacements of only some joints are expected to be controlled, and the remaining displacements will typically be free to take on any values, and similarly, the number of bar forces that exceed specified limits are also not typically large.

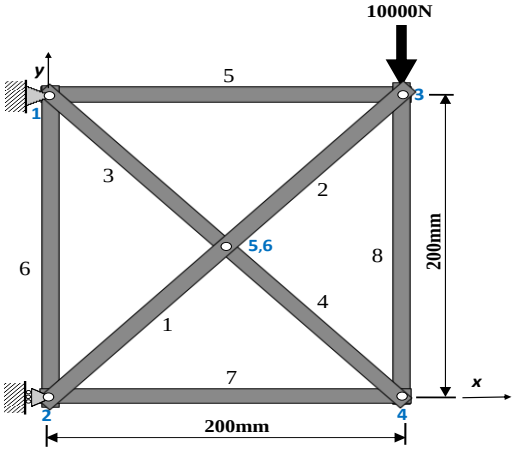

Fig. 2 A simple pantographic structure with three degrees of statical indeterminacy

2.5 An illustrative example of using Matrix Condensation in control

The procedure of displacement control without regard to bar forces, bar forces control without regard to displacements, and simultaneous displacement and bar force control by using condensed matrices in equations of control are now illustrated with the simple example pantographic structure as shown in Fig. 2. The structure has $EA=3.6\times10^5$ N and $EI=10.8\times10^5$ N.mm^2.

The example consists of a two-dimensional single unit pantograph, which is formed from two coplanar beams of equal length connected at their mid-point by frictionless shear connector, which is perpendicular to both beams. Four bars connect between adjacent ends of the pantograph. The structure has three states of selfstress as shown in Fig. 2. The technique of the reduced matrix is now applied to this example to find $\mathbf{A}^*$, $\mathbf{B}^*$ and $\mathbf{F}^*$. The original size of the equilibrium matrix is 18×24, and through using the condensation process (Kwan 1991, Pellegrino *et al.* 1992) the size of the given example reduces to 5×8 as shown below

$$\begin{bmatrix} -\frac{1}{\sqrt{2}} & 0 & -\frac{1}{2\sqrt{2}} & \frac{1}{2\sqrt{2}} & 0 & -1 & 0 & 0 \\ 0 & \frac{1}{\sqrt{2}} & \frac{1}{2\sqrt{2}} & -\frac{1}{2\sqrt{2}} & 1 & 0 & 0 & 0 \\ 0 & \frac{1}{\sqrt{2}} & -\frac{1}{2\sqrt{2}} & \frac{1}{2\sqrt{2}} & 0 & 0 & 0 & 1 \\ \frac{1}{2\sqrt{2}} & -\frac{1}{2\sqrt{2}} & 0 & \frac{1}{\sqrt{2}} & 0 & 0 & 1 & 0 \\ \frac{1}{2\sqrt{2}} & -\frac{1}{2\sqrt{2}} & 0 & -\frac{1}{\sqrt{2}} & 0 & 0 & 0 & -1 \end{bmatrix} \begin{bmatrix} t_1 \\ t_2 \\ t_3 \\ t_4 \\ t_5 \\ t_6 \\ t_7 \\ t_8 \end{bmatrix} = \begin{bmatrix} P_{2y} \\ P_{3x} \\ P_{3y} \\ P_{4x} \\ P_{4y} \end{bmatrix} \tag{39}$$

$$\overset{\uparrow}{\mathbf{A}}^* \qquad\qquad \overset{\uparrow}{\mathrm{t}}^* = \overset{\uparrow}{\mathrm{p}}^*$$

So the compatibility matrix satisfies Eq. (8) and the size of the matrix reduces from 24×18 to 8×5 as shown here.

$$\begin{bmatrix} -\frac{1}{\sqrt{2}} & 0 & 0 & \frac{1}{2\sqrt{2}} & \frac{1}{2\sqrt{2}} \\ 0 & \frac{1}{\sqrt{2}} & \frac{1}{2\sqrt{2}} & -\frac{1}{2\sqrt{2}} & -\frac{1}{2\sqrt{2}} \\ -\frac{1}{2\sqrt{2}} & \frac{1}{2\sqrt{2}} & -\frac{1}{2\sqrt{2}} & 0 & 0 \\ \frac{1}{2\sqrt{2}} & -\frac{1}{2\sqrt{2}} & \frac{1}{2\sqrt{2}} & \frac{1}{\sqrt{2}} & -\frac{1}{\sqrt{2}} \\ 0 & 1 & 0 & 0 & 0 \\ -1 & 0 & 0 & 0 & 0 \\ 0 & 0 & 0 & 1 & 0 \\ 0 & 0 & 1 & 0 & -1 \end{bmatrix} \begin{bmatrix} d_{2y} \\ d_{3x} \\ d_{3y} \\ d_{4x} \\ d_{4y} \end{bmatrix} = \begin{bmatrix} \mathbf{e}_{01}^{*} \\ \mathbf{e}_{02}^{*} \\ \mathbf{e}_{03}^{*} \\ \mathbf{e}_{04}^{*} \\ \mathbf{e}_{05}^{*} \\ \mathbf{e}_{06}^{*} \\ \mathbf{e}_{07}^{*} \\ \mathbf{e}_{08}^{*} \end{bmatrix} \tag{40}$$

$$\overset{\uparrow}{\mathrm{B}}^{*} \qquad \overset{\uparrow}{\mathrm{d}}^{*} = \overset{\uparrow}{\mathrm{e}}^{*}$$

Correspondingly, the flexible matrix reduces from 24×24 to 8×8

$$10^{-3} \times \begin{bmatrix} 436.87 & -436.49 & 0 & 0 & 0 & 0 & 0 & 0 \\ -436.49 & 436.87 & 0 & 0 & 0 & 0 & 0 & 0 \\ 0 & 0 & 436.87 & -436.49 & 0 & 0 & 0 & 0 \\ 0 & 0 & -436.49 & 436.87 & 0 & 0 & 0 & 0 \\ 0 & 0 & 0 & 0 & 0.56 & 0 & 0 & 0 \\ 0 & 0 & 0 & 0 & 0 & 0.56 & 0 & 0 \\ 0 & 0 & 0 & 0 & 0 & 0 & 0.56 & 0 \\ 0 & 0 & 0 & 0 & 0 & 0 & 0 & 0.56 \end{bmatrix} \begin{bmatrix} t_1 \\ t_2 \\ t_3 \\ t_4 \\ t_5 \\ t_6 \\ t_7 \\ t_8 \end{bmatrix} = \begin{bmatrix} \mathbf{e}_{o1}^{*} \\ \mathbf{e}_{o2}^{*} \\ \mathbf{e}_{o3}^{*} \\ \mathbf{e}_{o4}^{*} \\ \mathbf{e}_{o5}^{*} \\ \mathbf{e}_{o6}^{*} \\ \mathbf{e}_{o7}^{*} \\ \mathbf{e}_{o8}^{*} \end{bmatrix} \tag{41}$$

$$\overset{\uparrow}{\mathrm{F}}^{*} \qquad \overset{\uparrow}{\mathrm{t}}^{*} = \overset{\uparrow}{\mathrm{e}}^{*}$$

2.5.1 Controlling joint displacements only

The condensed displacements under non-zero load $\mathbf{d_{pc}}$ are as shown in Table 1 Column 4, and the structure deforms in such a way that the non-foundation joints 3 and 4 move to the right and downwards. For the controlling purpose, it is assumed that the nodal displacements in d_{3y} is to be restored to its original position zero displacement, i.e., we prescribe a levelling condition of the top of the structure, whilst the remaining displacement are free to take any value. All non-vanishing (i.e., uncondensed) $\mathbf{e_{no}}$ were chosen for actuation, since these bar elongations are actually possible and easy to effect (On the other hand, the condensed bar curvature would be a difficult actuation to practically effect). Since we are prescribing only one displacement, Eq. (33) has only one equation and becomes

$$\{0\} = \left\{ +\frac{1}{\sqrt{2}} \quad +\frac{1}{\sqrt{2}} \quad -\frac{1}{\sqrt{2}} \quad -\frac{1}{\sqrt{2}} \quad -\frac{1}{2} \quad -\frac{1}{2} \quad +\frac{1}{2} \quad +\frac{1}{2} \quad 0 \quad 0 \right\} \mathbf{e_{oc}} + \{-13.409\} \tag{42}$$

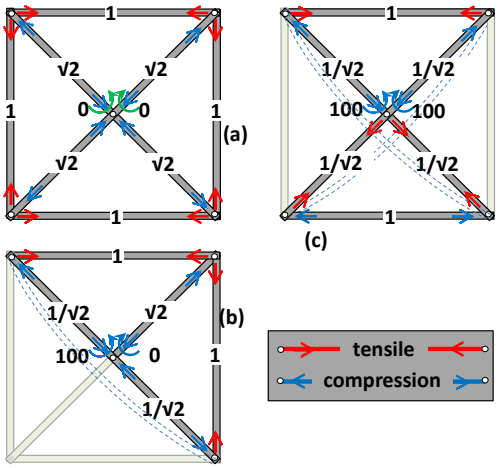

Fig. 3 Illustration of the three states of selfstress for the structure in Fig. 2 with exaggerated bending (-------) in the pantograph to show involvement by bending in the selfstress

which clearly has many possible solutions. One possible solution is to simply use the pseudoinverse to solve Eq. (42) since it is a common use to compute a 'best fit' (least squares) solution to a system of linear equations and its accuracy is enough for our purpose, where we thus obtain $\mathbf{e}_{oc} = \{+3.162\ +3.162\ -3.164\ -3.160\ -2.234\ -2.234\ +2.234\ +2.234\ 0\ 0\}^{T}$, Since the desired control displacement d_{3y} is one of the non-vanishing displacements and the actuation set of bars to control are non-vanished bar elongations $\mathbf{e}_{no}$, then Eq. (28), can also be used in this case, to give the same as, i.e., $\mathbf{e}_{no} = \{+3.162\ +3.162\ -3.164\ -3.160\ -2.234\ -2.234\ +2.234\ +2.234\}^{T}$, when this $\mathbf{e}_{no}$ is used as the corrective $\mathbf{e}_{oc}$, a displacement of 0.000 in d_{3y} as required does result, see Table 1 Column 5. Another useful impact is that all other displacements have also been reduced, in both *x* and *y* directions. However, the total elongation actuation (sum the absolute values of all member actuation) of the non-vanished bar elongations is 21.59mm, with eight separate actuations being used. Practically this is not a particular solution due to high member and amount of control in the non-vanishing bar elongations. For this purpose, we have to look for another set of $\mathbf{e}_{oc}$ which contains a fewer non-zero actuations, while still providing the target d_{3y}.

The best location of actuators should be decided at the design stage, so that structures can have actuators embedded for effective control of displacements under service loading. For recognition of which are the most effective bars to control d_{3y}, and the amount of required actuation, Eq. (42) must be used. The effectiveness of actuation in any bar is indicated by the size of the associated coefficient in the $\mathbf{Y}_c$ matrix in Eq. (42). Here, there two groups for effectual control of d_{3y}: firstly bars 1 to 4, and secondly, bars 5 to 8. The most effective actuation bars are those in the first group with the larger coefficients in $\mathbf{Y}_c$. The two elements of $\mathbf{Y}_c$ which vanish are the curvature of beam-pairs 1-5-3 and 2-6-4. For providing minimum actuation, we shall choose one of the four bars 1, 2, 3 and 4 for actuation since they have the largest coefficients in $\mathbf{Y}_c$ of Eq. (42). Even though each of the four bars, all with the large coefficients of $\mathbf{Y}_c$ in Eq. (42) has ability to control displacement of d_{3y} alone, the calculation was repeated for each of them in turn, with the results for each calculation shown Columns 6 to 9 in Table 1.

This was to check the displacement of all joints in both *x* and *y* directions after applying

Table 1 Displacements of the structure in Fig. 2 under different sets of $\mathbf{e}_{no}$

(1)	(2)	(3)	(4)	(5)	(6)	(7)	(8)	(9)
Joint	Cond. Disp.	Dir.	Just $\mathbf{d}_{pc}$, no $\mathbf{e}_{oc}$ (mm)	$\mathbf{Y}_c^{+}\mathbf{e}_{no}+\mathbf{d}_{pc}$ (mm)	Control with only $\mathbf{e}_{n1}$ (mm)	Control with only $\mathbf{e}_{n2}$ (mm)	Control with only $\mathbf{e}_{n3}$ (mm)	Control with only $\mathbf{e}_{n4}$ (mm)
1		*x*	0	0	0	0	0	0
		y	0	0	0	0	0	0
2		*x*	0	0	0	0	0	0
		y	-2.776	-0.543	-5.557	-5.549	+0.004	-0.002
3	$\mathbf{d}_m$	*x*	+2.776	+0.543	+5.549	+5.557	-0.004	+0.002
		y	**-13.409**	**0.000**	**0.000**	**0.000**	**0.000**	**0.000**
4		*x*	-2.776	-0.543	+0.005	-0.003	-5.547	-5.559
		y	-10.633	+0.543	+0.003	-0.005	+5.547	+5.559
5,6	$\mathbf{d}_p$	*x*	-1.387	-0.273	+6.701	-6.698	-9.469	+3.927
		y	-5.318	+0.273	+6.698	-6.701	+9.469	-3.927

required amount of actuation for each bar separately. For example, for bar 1, Eq. (42) becomes

$$\{0\}=\left\{ 1/\sqrt{2} \quad 0 \quad 0 \quad 0 \quad 0 \quad 0 \quad 0 \quad 0 \quad 0 \quad 0 \right\}\mathbf{e}_{oc}+\{-13.409\} \tag{43}$$

The use of the pseudoinverse on $\mathbf{Y}_c$ gives $\mathbf{e}_{oc}=\{\,18.963 \quad 0 \quad 0 \quad 0 \quad 0 \quad 0 \quad 0 \quad 0 \quad 0 \quad 0\}^{T}$. Similarly, the other calculations yields 18.963 for bar 2, -18.951 for bar 3, and -18.975 for bar 4.

As a result, comparison of the required amount of actuation in each of the four bars shows they are almost the same, and they all produce the target zero displacement of *dy3*. However, actuation in bar 4 does have advantage over other bars because, while all the other actuations produce similar displacements in joints 1 to 4, actuation in bar 4 does produce the least displacement in joint 5-6. This is principally because bar 4 is further remote from joint 5-6 to the support in joints 1 and 2, and hence shortening of bar 4 is not immediately displacing joint 5-6. In this way, the current approach can actually determine not only the necessary amount of actuation to be applied, but can also indicate the most effective bar(s) for a given set of displacement control.

2.5.2 Controlling bar forces only

For the purpose of controlling bar force without regarding to the joint displacements, firstly the bar forces $\mathbf{t}_{pc}$ under load are as shown in Table 2, Column 3. Structural members have a greater tendency for failure in compression than the tension, due to buckling in slender members, so it is presumed the need to control compression force in all members to a limit of -6000, whilst the tensile forces are free to take any value. Under the loading shown in Fig. 2, the given example has axial force in bars 1 and 2 ($\mathbf{t}_{n1}$ and $\mathbf{t}_{n2}$) exceeding the compression limit (see Column 3 in Table 2) with values of 7071.1.

In the first trial, all non-vanishing bar $\mathbf{e}_{no}$ were chosen for actuation since they are easily accessible for the actuation process (being bar length actuations rather than curvature). Only two bar forces are prescribed for control, which are those for bars 1 and 2 ($\mathbf{t}_{n1}$ and $\mathbf{t}_{n2}$), thus Eq. (37)

has only two equations, and becomes

$$\begin{bmatrix}-6000\\-6000\end{bmatrix}=\begin{bmatrix}\text{-373.4} & \text{-372.2} & \text{-372.8} & \text{-372.8} & 263.2 & 264.0 & 264.0 & 263.2 & 0 & 0\\ \text{-372.2} & \text{-373.4} & \text{-372.8} & \text{-372.8} & 264.0 & 263.2 & 263.2 & 264.0 & 0 & 0\end{bmatrix}\mathbf{e}_{\mathbf{oc}}+\begin{bmatrix}-7071.1\\-7071.1\end{bmatrix} \quad (44)$$

This system of course has many possible solutions. One possible solution process is to simply use the pseudoinverse to solve Eq. (44), which gives:

$$\mathbf{e}_{\mathbf{oc}}=\{-0.479\ -0.479\ -0.479\ -0.479\ +0.339\ +0.339\ +0.339\ +0.339\ 0\ 0\}^{\mathrm{T}}$$

Alternatively (and as also mentioned in Section 0), since t_{n1} and t_{n2} are among the non-vanishing $\mathbf{t_n}$ in this example, and the actuation is also among the non-vanishing bar elongations $\mathbf{e_{no}}$, then Eq. (35) can equally be used, giving the same results of $\mathbf{e_{no}}=\{-0.479\ -0.479\ -0.479\ -0.479\ +0.339\ +0.339\ +0.339\ +0.339\}^{\mathrm{T}}$ After using the corrective $\mathbf{e_{oc}}$ the force in bars 1 and 2 are reduced to -6000 as required, (see Table 2, Column 4) and at the same time, none of the other bars have compression force greater than 6000 and so, the objective condition is satisfied, and with a total actuation of 3.27 mm.

Observation of Eq. (44) shows that bars 1 to 4 have almost the same coefficients in $\mathbf{Z_c}$ in the two rows. Therefore, any effect $\mathbf{Z_c e_{oc}}$ has on each of bars 1 to 4 is the same for bars 1 and 2. In other words, the force in bars 1 and 2 can (only) be raised or lowered by the same amount, with actuation in any of bars 1 to 4. In this case, we can reduce the number of actuators from eight to two, thus we restrict the length actuators to just bars 1 and 2 (*i.e.* the same bars with force requiring control). As before, we shall seek to reduce the compressive force in bars 1 and 2 to -6000 for all bars. With the required $\mathbf{t_n}$ as -6000, the reduced Eq. (44) is

$$\begin{bmatrix}-6000\\-6000\end{bmatrix}=\begin{bmatrix}\text{-373.4} & \text{-372.2} & 0 & 0 & 0 & 0 & 0 & 0 & 0 & 0\\ \text{-372.2} & \text{-373.4} & 0 & 0 & 0 & 0 & 0 & 0 & 0 & 0\end{bmatrix}\mathbf{e}_{\mathbf{oc}}+\begin{bmatrix}-7071.1\\-7071.1\end{bmatrix} \quad (45)$$

which (through use of pseudoinverse) gives $\mathbf{e}_{\mathbf{oc}}=\{-1.437\ -1.437\ 0\ 0\ 0\ 0\ 0\ 0\ 0\ 0\}^{\mathrm{T}}$. This corrective $\mathbf{e_{oc}}$ is different to, and simpler than eno above, but, when applied, gives the same set of bar forces and also limits the force of bars 1 and 2 to -6000 as required, without any other bar force consequently exceeding the limit, see Table 2, Column 5. This time, the control is achieved with only 2.874mm as the total actuation of $\mathbf{e_{no}}$.

Actually, a further reduction in the number of actuators is possible this example by controlling the chosen bar forces $\mathbf{t_{n1}}$ and $\mathbf{t_{n2}}$ with only one actuator, since Eq. (44) shows that bars 1 to 4 have nearly the same coefficients in $\mathbf{Z_c}$. Therefore, any effect resulting from actuation in any of bars 1 to 4 has to be the nearly identical for both $\mathbf{t_{n1}}$ and $\mathbf{t_{n2}}$. If we choose bar alone for actuation, then Eq. (44) becomes

$$\begin{bmatrix}-6000\\-6000\end{bmatrix}=\begin{bmatrix}\text{-373.4} & 0 & 0 & 0 & 0 & 0 & 0 & 0 & 0 & 0\\ \text{-372.2} & 0 & 0 & 0 & 0 & 0 & 0 & 0 & 0 & 0\end{bmatrix}\mathbf{e}_{\mathbf{oc}}+\begin{bmatrix}-7071.1\\-7071.1\end{bmatrix} \quad (46)$$

and $\mathbf{e}_{\mathbf{oc}}=\{-2.873\ \ 0\ \ 0\ \ 0\ \ 0\ \ 0\ \ 0\ \ 0\ \ 0\ \ 0\}^{\mathrm{T}}$

Similarly, if we choose bar 2 for actuation, then reduced Eq. (44) becomes

$$\begin{bmatrix}-6000\\-6000\end{bmatrix}=\begin{bmatrix}0 & \text{-372.2} & 0 & 0 & 0 & 0 & 0 & 0 & 0 & 0\\ 0 & \text{-373.4} & 0 & 0 & 0 & 0 & 0 & 0 & 0 & 0\end{bmatrix}\mathbf{e}_{\mathbf{oc}}+\begin{bmatrix}-7071.1\\-7071.1\end{bmatrix} \quad (47)$$

Table 2 Bar forces of the structure in Fig. 2 under different sets of $\mathbf{e}_{no}$

(1)	(2)	(3)	(4)	(5)	(6)	(7)
Bar	Cond. Force	Just $\mathbf{t}_{pc}$, no $\mathbf{e}_{oc}$ (N)	All elements in $\mathbf{e}_{no}$ (N)	Control with only $\mathbf{e}_{n1}$ & $\mathbf{e}_{n2}$ (N)	Control with only $\mathbf{e}_{n1}$ (N)	Control with only $\mathbf{e}_{n2}$ (N)
1		**-7071.1**	**-6000.0**	**-6000.0**	**-5998.4**	**-6001.6**
2		**-7071.1**	**-6000.0**	**-6000.0**	**-6001.6**	**-5998.4**
3		+7075.6	+8146.6	+8146.6	+8146.6	+8146.6
4		+7066.6	+8137.6	+8137.6	+ 8137.6	+ 8137.6
5	$\mathbf{t}_n$	+4996.8	+4239.5	+4239.5	+4240.6	++4238.3
6		+4996.8	+4239.5	+4239.5	+4238.3	+4240.6
7		-4996.8	-5754.2	-5754.2	-5755.3	-5753.0
8		-4996.8	-5754.2	-5754.2	-5753.0	-5755.3
m(1,2)	$\mathbf{t}_p$	-635.7	-635.7	-635.7	-635.7	-635.7
m(3,4)		0.0	0.0	0.0	+232.5	-232.5

which again gives a similar $\mathbf{e}_{oc} = \{0 \quad -2.873 \quad 0 \quad 0 \quad 0 \quad 0 \quad 0 \quad 0 \quad 0 \quad 0\}^T$

The resultant bar forces from applying these two $\mathbf{e}_{oc}$ are calculated and collected in Columns 6 and 7 of the Table 2. Both columns show (near) identical results, so the force in bars 1 and 2 can actually be controlled via only one actuator. The principal difference in the two sets of resultant forces is in the moment of beam-pair 1-6-4 (i.e., m(3, 4)) which have values of -232.1 and +232.1. The difference results from $\mathbf{e}_{oc}$ having a shortening each time, in either bar 1 or in bar 2, but a shortening in bar 1 (which is "below" beam-pair 1-6-4) would bend that beam-pair in the opposite direction to a shortening in bar 2 (which is "above" that beam-pair). However, whether the beam-pair bends one way or the other, so long as the amount of bending is the same, then the effect at its pinned-ends (i.e., overall shortening) is the same, and hence the controlling effect on the rest of the structure is the same. This is why either Eq. (46) or Eq. (47) produces the same overall bar force effect (except for the moment m(3, 4)).

2.5.3 Simultaneously controlling joint displacement and bar force

The joint displacements and bar forces of the structure under load without any corrective actuation $\mathbf{e}_{oc}$ applied are shown together in Columns 4 and 5 of Table 3 respectively. We shall now impose both the controlling conditions introduced in the Subsections 0 and 0 simultaneously; so the nodal displacement in d_{3y} is to be zero (in order to keep the top of the structure level), and compression force in members are limited to -6000. Control is to be achieved through actuation in non-vanishing bar elongation $\mathbf{e}_{no}$, which we choose to be $\mathbf{t}_{n1}$ and $\mathbf{t}_{n2}$. Eq. (38) is now employed as a system of two equations in eight non-vanishing elongation unknowns

$$\begin{Bmatrix} 0 \\ -6000 \\ -6000 \end{Bmatrix} = \begin{Bmatrix} \mathbf{Y}_{c_{[\text{row 3, columns[1-8]}]}} \\ \mathbf{Z}_{c_{[\text{rows 1 and 2, columns[1-8]}]}} \end{Bmatrix} \mathbf{e}_{oc} + \begin{Bmatrix} -13.41 \\ -7071 \\ -7071 \end{Bmatrix} \tag{48}$$

Thus, Eq. (48) becomes

Table 3 Displacement and bar forces control of the structure in Fig. 2.

(1)	(2)	(3)	(4)	(5)	(6)	(7)	(8)	(9)	(10)	(11)
Jt	Cond. Disp.	Dir.	no $\mathbf{e}_{oc}$		$(\mathbf{e}_{oc})_1$		$(\mathbf{e}_{oc})_2$		Cond. Force	Bar
			$\mathbf{d}_{pc}$ (mm)	$\mathbf{t}_{pc}$ (N)	$\mathbf{d}_{pc}$ (mm)	$\mathbf{t}_{pc}$ (N)	$\mathbf{d}_{pc}$ (mm)	$\mathbf{t}_{pc}$ (N)		
1		*x*	0	**-7071**	0	**-6000**	0	**-6000**		1
		y	0	**-7071**	0	**-6000**	0	**-6000**		2
2		*x*	0	+7076	0	+8143	0	+8140		3
		y	-2.78	+7067	-0.46	+8141	-2.36	+8144		4
3	$\mathbf{d}_m$	*x*	+2.78	+4997	0.46	+4242	+2.36	+4244	t_n	5
		y	**-13.41**	+4997	**0.00**	+4242	**0.00**	+4244		6
4		*x*	-2.78	-4997	-0.63	-5757	-3.20	-5759		7
		y	-10.63	-4997	+0.63	-5757	+3.20	-5759		8
5,6	$\mathbf{d}_p$	*x*	-1.39	-636	-0.31	-125	+2.26	+248	t_p	m(1,2)
		y	-5.32	0	+0.31	0	-2.26	0		m(3,4)

(Displacements (shaded) and bar forces (unshaded) of the structure: with no $\mathbf{e}_{oc}$; with $(\mathbf{e}_{oc})_1$ and $(\mathbf{e}_{oc})_2$ applied to adjust the controlled displacements (Column 4) and bar forces (Column 5) shown in bold)

$$\begin{Bmatrix} 0 \\ -6000 \\ -6000 \end{Bmatrix} = \begin{Bmatrix} +0.707 & +0.707 & -0.707 & -0.707 & -0.500 & -0.500 & +0.500 & +0.500 & 0 & 0 \\ -373.4 & -372.2 & -372.8 & -372.8 & +263.2 & +264.0 & +264.0 & +263.2 & 0 & 0 \\ -372.2 & -373.4 & -372.8 & -372.8 & +264.0 & +263.2 & +263.2 & +264.0 & 0 & 0 \end{Bmatrix} \mathbf{e}_{oc} + \begin{Bmatrix} -13.41 \\ -7071 \\ -7071 \end{Bmatrix} \quad (49)$$

Simply through the pseudoinverse of the 3×8 compound matrix $[\mathbf{Y}_c|\mathbf{Z}_c]^T$ a set of actuation obtained as: $(\mathbf{e}_{oc})_1 = \{\, 2.683 \;\; 2.683 \;\; -3.643 \;\; -3.638 \;\; -1.896 \;\; -1.896 \;\; 2.573 \;\; 2.573 \;\; 0 \;\; 0 \,\}^T$

Table 3 shows the effects of $(\mathbf{e}_{oc})_1$ in Columns 6 and 7, and that all the required controls are achieved, without any introduction of a new bar force compression violation. The total amount of actuation required by $(\mathbf{e}_{oc})_1$ is 21.585 mm.

The coefficients in Eq. (49) also identify which are the most effective bars for a given set of simultaneous displacement and bar force control. The minimum number of actuations to deliver the required displacements and bar forces can obtained by choosing the bars corresponding to the biggest coefficients of $[\mathbf{Y}_c|\mathbf{Z}_c]^T$. In this example, we thus choose the three most effective bars, instead of all eight, for actuation, and these are bars 1, 2 and 4. Bar 4 was chosen for control of d_{3y} (following the large coefficients for $\mathbf{Y}_c$) and bars 1 and 2 were chosen for $\mathbf{t}_{n1}$ and $\mathbf{t}_{n2}$ respectively (following the large coefficients for $\mathbf{Z}_c$). Therefore. Therefore, Eq. (49) simplified to

$$\begin{Bmatrix} 0 \\ -6000 \\ -6000 \end{Bmatrix} = \begin{Bmatrix} 0.7071 & +0.7071 & 0 & -0.7067 & 0 & 0 & 0 & 0 & 0 & 0 \\ -373.4 & -372.2 & 0 & -372.8 & 0 & 0 & 0 & 0 & 0 & 0 \\ -372.2 & -373.4 & 0 & -372.8 & 0 & 0 & 0 & 0 & 0 & 0 \end{Bmatrix} \mathbf{e}_{oc} + \begin{Bmatrix} -13.41 \\ -7071 \\ -7071 \end{Bmatrix} \quad (50)$$

and $(\mathbf{e}_{oc})_2 = \{+4.024 \;\; +4.024 \;\; 0 \;\; -10.921 \;\; 0 \;\; 0 \;\; 0 \;\; 0 \;\; 0 \;\; 0\}^T$

This reduced set of $\mathbf{e}_{oc}$ satisfies both displacement and bar force condition without any bar violations, as shown in Columns 8 and 9 of Table 3. At the same time, not only is the total number

of actuators reduced from eight to three, but the total amount of actuation has also reduced, from $(\mathbf{e}_{oc})_1$=21.585 mm to $(\mathbf{e}_{oc})_2$=18.970 mm. There has thus been a double advantage in using Eq. (50).

As a result, it is proven in this Section that linear controlling equations using condensed matrix is as powerful as using non-condensed matrix for control or adjustments of structural shape and/or force. Moreover, these equations can be used in finding controlling displacement and bar force with minimum actuation, as well as in cases where the actuator locations are already fixed. The same set of equations derived in this Section are also applicable for shape adjustment of structures containing macro-elements (i.e., elements built up from one or more fundamental elements), of which the pantograph element used in Fig. 2 is only one example.

3. Comparison the current method with previous techniques

The purpose of this paper is controlling nodal displacement and/or internal bar force control of for structures made up of more complex structural components (i.e., those with "macro-elements"), e.g., the pantographic. Since work on the associated analytical/computational techniques on these types of structure is rare and this technique is valid for noncomplex structures as well, so the present technique was applied on a simple pin-jointed assembly under load as shown in Fig. 4 and compared with results previously published by You (1997), Shen *et al.* (2006) as cited by Xu and Luo (2008) and Xu and Luo (2008) who worked on displacement control of a prestressed 9-cable network structure as shown in Fig. 4, where all cables have axial stiffness (EA) of 43.16 kN. The prestress of the structure (You 1997) is shown in Column 4 of Table 4, which is produced by changing the length of the cables vii, viii, and ix by the amounts of -5.02 mm, +4.49 mm and -5.52 mm respectively. The consequent displacements for these actuations are shown in Column 3. You (1997) set the target displacement for control as negation of the displacement of node 6, which has pre-adjustment displacements of $[2.56, -4.31]^T$ mm, and this was to be changed to $[0, 0]^T$. Furthermore, the condition was also given that the internal force of the cables had to be kept above their initial values i.e., $\mathbf{t} \geq \mathbf{t}_o$.

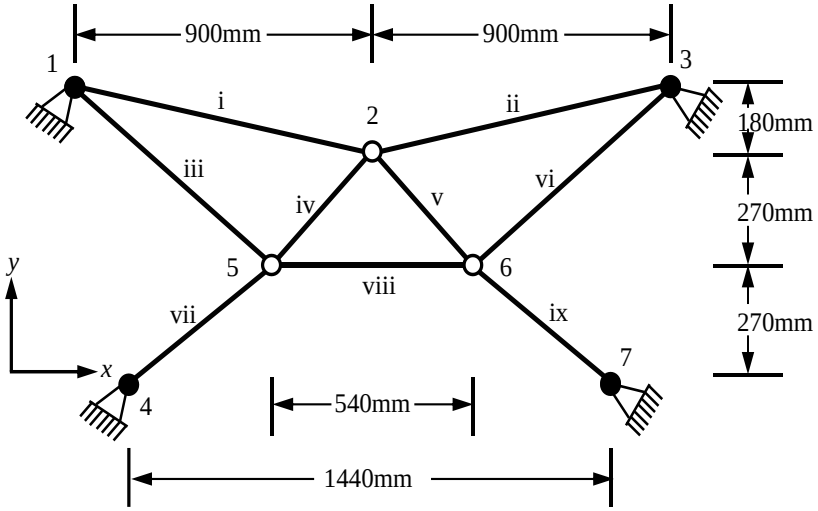

Fig. 4 A plane cable net structure (You 1997)

Table 4 Comparison the present technique of linear shape control with You, Shen and Xu techniques for linear shape control of cable net structure in Fig. 4

(1)	(2)	(3)	(4)	(5)	(6)	(7)	(8)	(9)	(10)	(11)	(12)	(13)	(14)	(15)	(16)	(17)
Joint	Dir	Pre-adjustment		Post-adjustment (Theoretical)												Member
		Theoretical		**You ***			**Present study***			**Shen***	**Present study**			**Shen**	**Xu**	
		d_o (mm)	**t_o** (N)	**D** (mm)	**T** (N)	**e_o** (mm)	**D** (mm)	**T** (N)	**e_o** (mm)	**e_o** (mm)	**D** (mm)	**T** (N)	**e_o** (mm)	**e_o** (mm)	**e_o** (mm)	
2	*x*	0.00	61.38	0.29	141.8	0.00	-0.02	117.48	0.00	0.00	-1.05	61.38	-1.72	-1.72	-2.56	1
	y	-6.66[+]	61.38	-0.60	115.0	0.00	-12.82	118.84	0.00	0.00	-3.13	61.38	0.34	0.34	0.00	2
5	*x*	-2.56[+]	23.55	-0.21	33.3	0.00	-5.22	23.55	0.00	0.00	-3.24	23.55	-1.38	-1.38	0.00	3
	y	-4.31	17.02	-8.50	17.0	0.00	-8.03	33.71	0.00	0.00	-2.90	17.02	1.24	1.24	0.02	4
6	*x*	**2.56**	17.02	**0.00**	54.1	-10.53	**0.00**	31.83	-9.33	-8.90	**0.00**	17.02	-1.62	-1.62	-2.44	5
	y	**-4.31**	23.55	**0.00**	23.5	-0.42	**0.00**	24.05	-0.43	-0.57	**0.00**	23.55	-0.42	-0.42	-0.63	6
			50.00		61.1	-4.67		72.94	-4.47	-4.83		50.00	0.14	0.14	-0.01	7
			50.00		67.5	0.00		57.87	0.00	0.00		50.00	-1.88	-1.88	-3.09	8
			50.00		101.1	3.79		70.91	4.16	4.30		50.00	4.41	4.41	4.21	9
		total actuation (mm)				19.41			18.39	18.60		13.15		13.15	12.96	

*These three solutions have assumed that only the cables no. 5-9 are adjustable.
+These numbers have been corrected due to a sign omission in the original (You 1997)

The set of results are achieved via two alternative sets of actuator. The first set assumed that only the cables 5 to 9 are adjustable, while in the second set, all cables were allowed to participate in the adjustment process for achieving the required target. Firstly, following You's original work in only actuating cables 5 to 9, the displacements and internal bar forces after adjustment from using the present method, are shown in Columns 8 and 9 of Table 4. The set of actuation calculated (Column 10) is slightly different to that given by You (Column 7) and Shen *et al.* (Column 11), and a slightly smaller total actuation than both previous methods have also been achieved. All three methods attained the target of both eliminating displacements of node 6 (Columns 5 and 8) without any decrease in any of the cable forces. Secondly, when Shen *et al.* (2006) studied this example, they also allowed all cables to be actuated, and the post-adjustment displacement and cable force results from the present method, are shown in Columns 12 and 13 of Table 4, which shows again that the target control was achieved. In actual fact, the present technique found the same set of actuation found by Shen *et al.* (2006) (Column 15) while Xu and Luo (2008) found a slightly different set of actuator (Column 16) which had a slightly smaller total actuation.

4. Conclusions

A useful and relatively simple method has been presented in this paper which provides a direct method for calculating required length actuations for structures made up of more complex structural components (i.e., those with "macro-elements"), e.g., the pantographic element requiring shape or force control, or both. This technique involved structural matrices being built up from

matrices of elementary elements, and then processed with "matrix condensation". The advantages of the method is that the changes for both force and displacement regimes are within a single formulation, and preference is given to solutions which involve a minimal number of length actuation and also minimal amount of actuations. It was concluded that the proposed system performs well in seeking the optimal set for the shape control of prestressed structures through comparison of this study with other techniques.

References

Burdisso, R.A. and Haftka, R.T. (1990), "Statistical analysis of static shape control in space structures", *AIAA J*., **28**(8), 1504-1508.

Du, J., Bao, H. and Cui, C. (2014), "Shape adjustment of cable mesh reflector antennas considering modeling uncertainties", *Acta Astronautica*, **97**, 164-171.

Du, J., Zong, Y. and Bao, H. (2013), "Shape adjustment of cable mesh antennas using sequential quadratic programming", *Aerosp. Sci. Tech*., **30**(1), 26-32.

Edberg, D.L. (1987), "Control of flexible structures by applied thermal gradients", *AIAA J*., **25**(6), 877-883.

Hadjigeorgiou, E.P., Stavroulakis, G.E. and Massalas, C.V. (2006), "Shape control and damage identification of beams using piezoelectric actuation and genetic optimization", *Int. J. Eng. Sci*., **44**(7), 409-421.

Haftka, R.T. and Adelman, H.M. (1985a), "An analytical investigation of shape control of large space structures by applied temperatures", *AIAA J*., **23**(3), 450-457.

Haftka, R.T. and Adelman, H.M. (1985b), "Selection of actuator locations for static shape control of large space structures by heuristic integer programing", *Comput. Struct.*, **20**(1), 575-582.

Irschik, H. (2002), "A review on static and dynamic shape control of structures by piezoelectric actuation", *Eng. Struct.*, **24**(1), 5-11.

Kawaguchi, K.I., Hangai, Y., Pellegrino, S. and Furuya, H. (1996), "Shape and stress control analysis of prestressed truss structures", *J. Reinf. Plast. Compos.*, **15**(12), 1226-1236.

Korkmaz, S. (2011), "A review of active structural control: challenges for engineering informatics", *Comput. Struct.*, **89**(23), 2113-2132.

Kwan, A.S.K. (1991), "A pantographic deployable mast", PhD Thesis, University of Cambridge, Cambridge, UK.

Kwan, A.S.K. and Pellegrino, S. (1993), "Prestressing a space structure", *AIAA J*., **31**(10), 1961-1963.

Kwan, A.S.K. and Pellegrino, S. (1994), "Matrix formulation of macro-elements for deployable structures", *Comput. Struct.*, **50**(2), 237-254.

Mitsugi, J., Yasaka, T. and Miura, K. (1990), "Shape control of the tension truss antenna", *AIAA J*., **28**(2), 316-322.

Pellegrino, S. (1993), "Structural computations with the singular value decomposition of the equilibrium matrix", *Int. J. Solid. Struct.*, **30**(21), 3025-3035.

Pellegrino, S., Kwan, A.S.K. and Van Heerden, T.F. (1992), "Reduction of equilibrium, compatibility and flexibility matrices, in the force method", *Int. J. Numer. Meth. Eng.*, **35**(6),1219-1236.

Saeed, N.M. (2014), "Prestress and deformation control in flexible structures", PhD Thesis, Cardiff University, Cardiff, UK.

Salama, M., Umland, J., Bruno, R. and Garba, J. (1993), "Shape adjustment of precision truss structures: analytical and experimental validation", *Smart Mater. Struct.*, **2**(4), 240.

Shea, K., Fest, E. and Smith, I.F.C. (2002), "Developing intelligent tensegrity structures with stochastic search", *Adv. Eng. Inform.*, **16**(1), 21-40.

Shen, L.Y., Li, G.Q. and Luo, Y.F. (2006), "Displacement control of prestressed cable structures", *J. Tongji Univ. Nat. Sci.*, **34**(3), 291-295. (in Chinese)

Subramanian, G. and Mohan, P. (1996), "A fast algorithm for the static shape control of flexible structures",

Comput. Struct., **59**(3), 485-488.
Sunar, M. and Rao, S.S. (1999), "Recent advances in sensing and control of flexible structures via piezoelectric materials technology", *Appl. Mech. Rev.*, **52**(1), 1-16.
Tanaka, H. (2011), "Surface error estimation and correction of a space antenna based on antenna gainanalyses", *Acta Astronautica*, **68**(7), 1062-1069.
Tanaka, H. and Natori, M. (2006), "Shape control of cable-network structures based on concept of self-equilibrated stresses", *JSME Int. J. Ser. C*, **49**, 1067-1072.
Tanaka, H. and Natori, M.C. (2004), "Shape control of space antennas consisting of cable networks", *Acta Astronautica*, **55**(3), 519-527.
Trak, A.B. and Melosh, R.J. (1992), "Passive shape control of space antennas with truss support structures", *Comput. Struct.*, **45**(2), 297-305.
Wang, Z., Chen, S.H. and Han, W. (1997), "The static shape control for intelligent structures", *Finite Elem. Anal. Des*., **26**(4), 303-314.
Wang, Z., Li, T. and Cao, Y. (2013), "Active shape adjustment of cable net structures with PZT actuators", *Aerosp. Sci. Tech.*, **26**(1), 160-168.
Xu, X. and Luo, Y.Z. (2008), "Multi-objective shape control of prestressed structures with genetic algorithms", *Proceedings of the Institution of Mechanical Engineers, Part G: Journal of Aerospace Engineering*, **222**(8), 1139-1147.
Yang, S. and Ngoi, B. (2000), "Shape control of beams by piezoelectric actuators", *AIAA J*., **38**(12), 2292-2298.
You, Z. (1997), "Displacement control of prestressed structures", *Comput. Meth. Appl. Mech. Eng.*, **144**(1), 51-59.
Yu, Y., Zhang, X.N. and Xie, S.L. (2009), "Optimal shape control of a beam using piezoelectric actuators with low control voltage", *Smart Mater. Struct.*, **18**(9), 095006.
Ziegler, F. (2005), "Computational aspects of structural shape control", *Comput. Struct.*, **83**(15), 1191-1204.

CC